Performance comparison of inkjet and thermal transfer printed passive ultra-high-frequency radio-frequency identification tags

Journal Item

Performance Comparison of Inkjet and Thermal Transfer Printed Passive UHF RFID Tags

Monageng Kgwadi[1], Muhammad Rizwan[2], Ajith Adhur Kutty[2], Johanna Virkki[2], Leena Ukkonen[2], Timothy D. Drysdale[3,*]

[1]Electronics and Nanoscale Engineering Division, University of Glasgow, G12 8QQ, UK.

[2]Department of Electronics and Communications Engineering, Tampere University of Technology, Tampere, Finland.

[3]Department of Engineering and Innovation, The Open University, Milton Keynes, MK7 6AA, UK.

[*]tim.drysdale@open.ac.uk

Abstract: We compare the maximum read range of passive ultra high frequency (UHF) radio frequency identification (RFID) tags that have been produced using different metal printing techniques, specifically inkjet printing and thermal transfer printing. We used the same substrate (THERMLfilm), antenna designs, and electronic circuitry in our comparison so as to isolate the effect of the metal printing. Due to the high metal conductivity, the thermal transfer printed tags printed with copper ink performed as well or better than the inkjet printed tags printed with silver ink, even when we changed the inkjet printed tags to a Kapton substrate that is better suited to inkjet printing. The aluminium thermal transfer printed tags had up to 33% less read range than copper thermal transfer printed tags. Thermal transfer printing needs no sintering, and provides an attractive alternative low-cost fabrication method. Characterisation of the printed traces by both methods reveals that the printing techniques achieve similar surface roughness between 19.8 nm and 21.2 nm RMS. The achieved conductivities for thermal transfer printing on THERMLfilm were 2.6×10^7 S/m and 3.9×10^7 S/m for aluminium and copper films respectively while inkjet printing achieved 1.7×10^7 S/m conductivity on the same substrate. The best measured read range

for THERMLfilm was 10.6m . Across the different tag designs, the measured read ranges were 15-60% (1-10%) better for thermal printing, compared to inkjet printing on THERMLfilm (Kapton).

1. Introduction

The drive to develop low-cost, flexible and lightweight electronics to support Internet of Things (IoT) applications has received a lot of attention in recent years [1]. The IoT is envisaged to consist ultimately of trillions of communicating devices operating in diverse applications such as smart cities, personal area networks, smart homes, supply chain management, and smart grids [2, 3, 4, 5] to name but a few. Pervasive adoption of IoT application hinges on a low unit cost for the nodes [6], hence the need to develop low-cost manufacturing of electronics by both academia and industry [3, 4].

A number of inexpensive techniques are available for printing electronics. These include additive methods such as inkjet printing (e.g. of antennas [7], frequency selective surfaces [8], UHF passive components[9], sensors [10] and circuits [11]) and screen printing (e.g. of electronic circuits [12] and passive sensors [13]). Both are well known and widely used approaches to deposit an ink containing conductive particles or flakes typically metallic, which then requires sintering to achieve the maximum available conductivity. Nonetheless, newer developments may from time to time emerge, potentially offering improved processing methods that are faster, more convenient and less expensive. One such development is the introduction of metal ribbons for thermal transfer printing (TTP), which has enabled the printing of antennas [14] and frequency selective surfaces [15] without the need for a sintering step (which is essential in inkjet printing). On the other hand, the metal thickness available through thermal transfer printing appears relatively thin (ca. 300 nm) compared with inkjet printed metal thicknesses which can be over 1 μm. This difference would appear to be critical to the operation of a UHF RFID tag where the skin depth is $\sim$2 μm in pure copper at 1 GHz [16], yet the quality of the deposited metal (represented by its conductivity or sheet resistance) is also a determining factor, as is the influence of substrate on the adhesion of the ink, surface roughness, loss and mechanical flexibility [17, 18]. In this paper, we seek to compare

the overall performance obtained by designing a set of three UHF RFID tags with different antennas that use a representative mixture of thick and thin line widths, printing them using both inkjet and thermal transfer printing on the same substrate, and then determining from measurements, the maximum read range. In this paper we confine our interest to a subset of printing techniques (inkjet and thermal transfer) that can support individually customised designs, so we do not consider the relative performance of screen printing. Inkjet and screen printing have already been benchmarked against each other, e.g. [19]. To the best of our knowledge, this is the first systematic comparison of thermal transfer printed UHF RFID antennas to either.

The paper is organised as follows; the printing techniques and the equipment used in this study are discussed in Section 2. Physical and electrical characterisation of the traces of the two methods are discussed in Section 3. The UHF RFID tag designs used in this study and the evaluation method are discussed in Section 4. Section 5 presents the simulated read range of the tags while Section 6 presents results of the measurements. Conclusions are then drawn in Section 7.

2. Methods

We wish to compare the effect of changing the technique for printing the metal antennas and circuit traces, so we keep the rest of the tag as similar as possible. In particular, to use the same antenna designs, the same electronic circuit, and the same substrate. The use of the same substrate allows us to eliminate sources of variation arising from differences in the thickness, dielectric constant, dielectric loss, and surface roughness. The only substrate available to us that could achieve consistent results using both techniques was THERMLfilm SELECT 21944E, formerly known as TC-390, from Flexcon.

For brevity, we refer to this substrate as THERMLfilm in the rest of the paper. THERMLfilm is a 50 μm thick polyester based flexible substrate with a glossy finish backed with a 20 μm thick acrylic adhesive and a removable 56 μm thick glassine liner suitable for TTP [20]. The relative dielectric constant of THERMLfilm SELECT 21944E is $\epsilon_r = 3.2$ [15]. THERMLfilm is best

suited to thermal transfer printing, and has a porous surface that absorbs a fraction of the ink when deposited using inkjet printing. This leads to the spreading of the ink drops and thinning of the metalisation which is expected to slightly degrade the performance of the inkjet printed tags, as discussed in Ref. [21]. So we can estimate the impact of the THERMLfilm porosity on inkjet printing, we also inkjet print onto Kapton, which has negligible absorption and is well suited to inkjet printing.

2.1. Inkjet Printing

For this work, we used a Fujifilm Dimatix DMP-2831 material inkjet printer, with 10 pL print nozzles. The ink was Harima's NPS-JL silver nanoparticle ink with particle sizes of 5-12 nm with a maximum achievable conductivity in the range of 1.6×10^7 - 2.5×10^7 S/m [22]. We chose this ink because it is commonly used, but we note other (potentially more cost-effective) metallic inks are available and under development [23]. The optimized inkjet printing key parameters are presented in Table 1. Four of the sixteen jets were used simultaneously to obtain continuous traces on THERMLfilm at a jetting voltage of 28 V and a cartridge temperature of 40 ^{o}C. A high platen temperature (60 ^{o}C) was used to reduce ink drying time. After printing, the sample was left on the platen for between two and three minutes so as to partially dry the ink. The samples were then sintered for one hour at 150 ^{o}C.

Table 1 Inkjet Printing Key Parameters

Parameter	**value**
Platen Temperature	60 ^{o}C
Cartridge Temperature	40 ^{o}C
Max. Jetting Frequency	9 KHz
Jetting Voltage	28 V
Drop Velocity	8-9 m/s
Drop Volume	10 pL
Drop Spacing/Pattern resolution	40 μm/635 DPI

2.2. Thermal Transfer Printing

Thermal transfer printing employs a multi-layered ribbon containing a prepared ink layer. For metal printing, the ribbon features a plastic membrane on top of which a thin layer of metal is

bonded using a resin, and a heat-sensitive acrylic adhesive on top of the metal. Printing is achieved by using a thermal print-head to selectively activate the desired regions of the heat-sensitive adhesive which then adheres to a substrate placed in physical contact with the ribbon and in the process, transfers the thin metal from the ribbon to the substrate as shown by Fig. 1*a*. We use two different IIMAK Metallograph^{TM} Conductive Thermal Transfer Ribbons (CTTR). One ribbon had a 260 nm thick aluminium film while the other has 340 nm thick copper film and both have a 1 μm thick heat-sensitive acrylic adhesive. A schematic of the Zebra S4M thermal printer used is shown in Fig. 1*b* showing the operation of the printer, while a photograph of the printer is shown in Fig. 1*c*. The printer has a print-head resolution of 300 dpi and a print speed of 5 cm/s. The sample can be used immediately with no drying or curing required.

Table 2 Metallograph ribbon : key parameters

Metal	Aluminium	Copper
Metalisation thickness	260 nm	340 nm
Adhesive thickness	1 μm	1 μm

3. Print Characterisation

We note that multi-layer printing techniques are available for each type of printing, but are not equally mature. Hence we confine our present study to single layer printing. Before producing the UHF RFID tags, we characterised traces printed using both methods.

3.1. Inkjet Printing

Inkjet printing produces continous traces on THERMLfilm when using the parameters in Table 1. As shown in Fig. 2*a* , a white light microscope image of the printed trace shows some small discontinuities in the printed traces, which could be caused by air bubbles forming during jetting, dust or sintering artifacts. Current scattering due to surface roughness is known to cause up to 40% increase the resistivity of thin films [24], which inevitably results in increased ohmic losses in antennas, and lower read ranges for the UHF RFID tags that we consider in this paper. A surface roughness measurement of a trace was made using a Bruker Dimension Icon atomic force

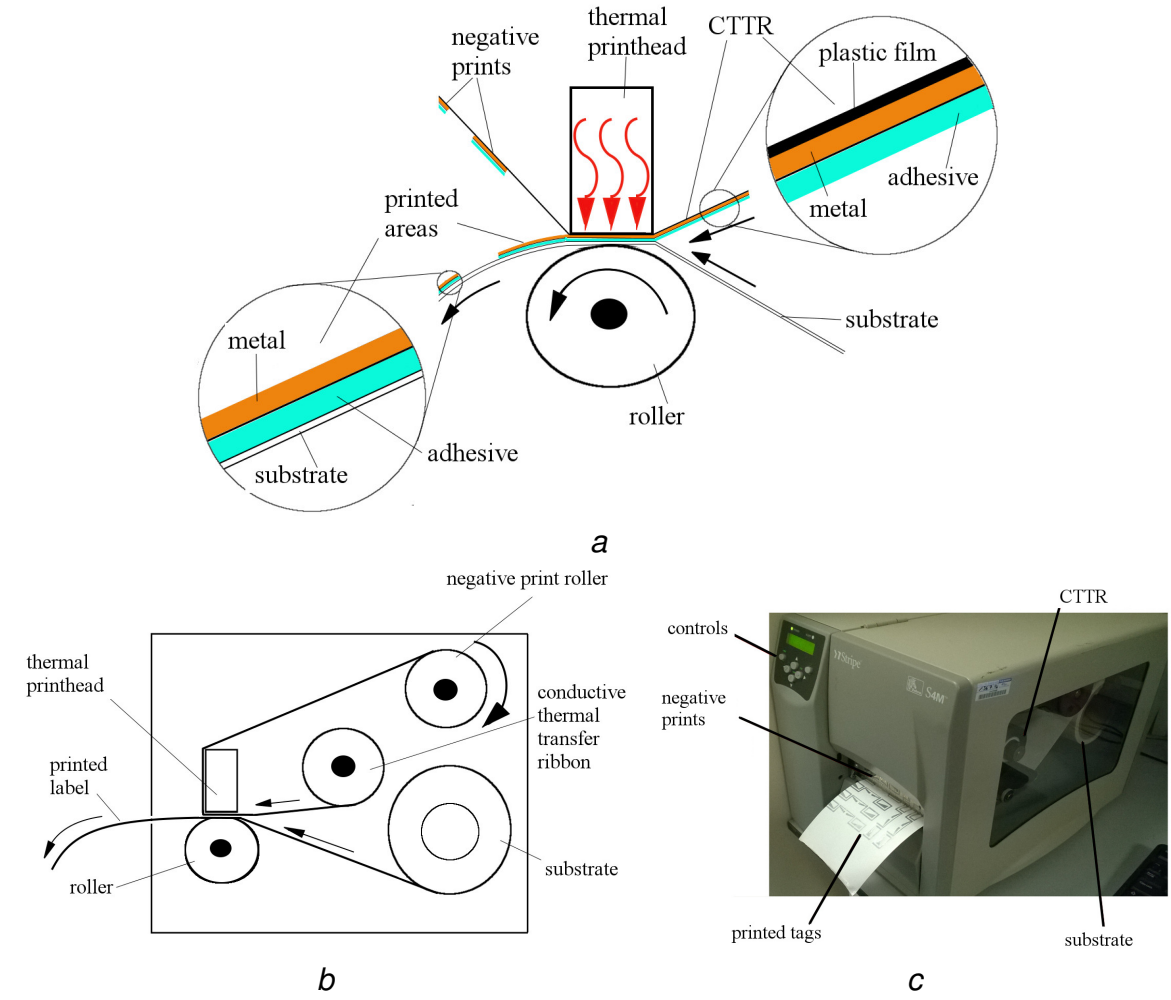

Fig. 1. *Thermal printing process*
a Schematic of the printing method
b Schematic of the Zebra S4M printer
c Photograph of the Zebra S4M printer

microscope (AFM) on an area of 5×2 μm that was representative of the sample and is shown in Fig. 2*b*. The measured root mean square (RMS) surface roughness was 21.2 nm, which is comparable to the measurements in [19] of 22.1 nm (RMS) inkjet printing on Polyetherimide (PEI), a substrate well suited for inkjet printing. THERMLfilm substrate has a measured surface roughness of 26.5 nm (RMS).

The thickness of the metal traces was measured using a Veeco Wyko NT1100 optical profiler to be in the range of 0.40-0.60 μm. The measured sheet resistance of the silver inkjet traces on

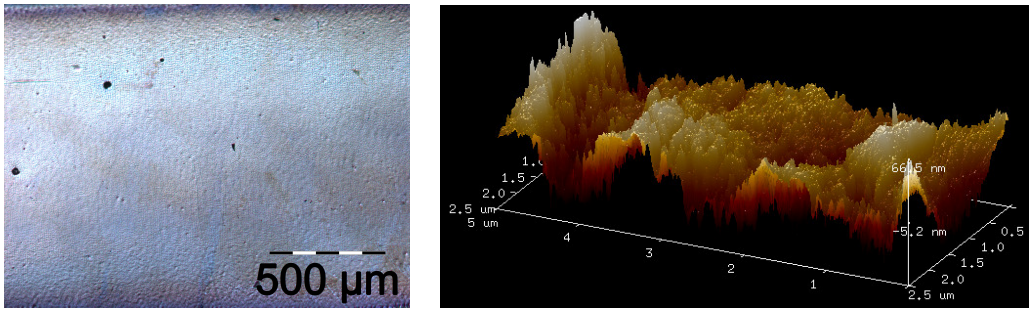

Fig. 2. *Physical characteristics of thermal transfer printed traces*
a Microscope image of inkjet trace on THERMLfilm
b AFM image of inkjet trace on THERMLfilm. Note that the trace edges are outside the edge of the pictures, and that the AFM trace covers $\sim 1/100^{th}$ of the the area shown

THERMLfilm using the four probe method on Agilent's B1500 Semiconductor Device Analyzer with American Probe & Technologies' Quasi Kelvin Probes was 0.15 $\Omega/\square$. We calculated conductivity using the average metal thickness and sheet resistance to be 1.7×10^7 S/m. The calculated skin depth for inkjet on THERMLfilm at 900 MHz is 4.1 μm. For comparison, the realized metal thickness on Kapton was 1.0 μm while the measured sheet resistance was 0.056 $\Omega/\square$, yielding conductivity of 1.8×10^7 S/m. The skin depth of inkjet on Kapton is 3.9 μm at 900 MHz. Thus the metalisation is 12.9% of the skin depth for inkjet printed traces on THERMLfilm, while it is 25.6% on Kapton. Therefore larger ohmic losses are expected on the inkjet printed traces on THERMLfilm than on Kapton.

3.2. Thermal Transfer Printing

White light optical microscope images of thermal transfer printed metal traces are shown in Fig. 3 with aluminium in Fig. 3*a* and copper in Fig. 3*b*. The images photos show hairline discontinuities on both the aluminium and copper traces. The discontinuities are more clearly shown in the aluminium trace due to the contrast in the picture but the density is higher in the copper traces ($\sim 8/\text{mm}^2$). We attribute these discontinuities to mechanical stresses associated with the handling of this prototype material, although further investigations are required to characterise the mechanism and are outside the scope of this paper.

The sheet resistance of the thermally printed traces on THERMLfilm was measured by the four probe method. The results are summarised in Table 3. The sheet resistance measured for both copper and aluminium traces shows a small dependence on the direction of print. This is attributed to the print elements being positioned in a single line across the width of the print substrate, perpendicular to the direction of substrate movement. The aluminium traces have a measured sheet resistance of 0.16 $\Omega/\square$ along print direction and 0.15 $\Omega/\square$ across the print direction. Copper traces have a measured sheet resistance of 0.10 $\Omega/\square$ along the print direction and 0.08 $\Omega/\square$ across the print direction. Thus the highest conductivity of the aluminium and copper traces are 2.6×10^7 S/m and 3.9×10^7 S/m respectively. The calculated skin depth at 900 MHz for aluminium and copper on THERMLfilm is 3.4 μm and 3.1 μm respectively, yielding a metalisation thickness that is 8.4 % and 12.6 % of the skin depth respectively. Therefore the copper tags are expected to have a higher read range than the aluminium tags.

An AFM surface roughness measurement of both traces was made on an area of 5×5 μm. The surface roughness of the aluminium and copper traces are shown in Fig. 4*a* and Fig. 4*b* respectively. The aluminium traces had an RMS roughness of 20.8 nm while the copper traces have an RMS roughness of 19.8 nm. The copper traces have a marginally smoother surface than aluminium with 0.4 nm average (1.0 nm rms). Both the aluminium and copper traces have a slightly smoother surface roughness than the inkjet traces on THERMLfilm (21.2 nm) and the surface roughness reported in [19].

Table 3 Key physical and DC characteristics of inkjet and TTP. Note that TTP sheet resistance and conductivity results are reported both perpendicular ($\perp$) and parallel ($\|$) to the direction of substrate movement

	Inkjet THERMLfilm	TTP Aluminium THERMLfilm	TTP Copper THERMLfilm	Inkjet Kapton
Metal Thickness	400-600 nm	260 nm	340 nm	1 μm
Surface Roughness (RMS)	21.2 nm	20.8 nm	19.8 nm	-
Sheet Resistance	0.15 $\Omega/\square$ -	0.15 $\Omega/\square$ $\perp$ 0.16 $\Omega/\square$ $\|$	0.08 $\Omega/\square$ $\perp$ 0.10 $\Omega/\square$ $\|$	0.056 $\Omega/\square$ -
Conductivity	1.7×10^7 S/m	2.6×10^7 S/m	3.9×10^7 S/m	1.8×10^7 S/m
Skin Depth at 900 MHz	4.1 μm	3.4 μm	3.1 μm	3.9 μm

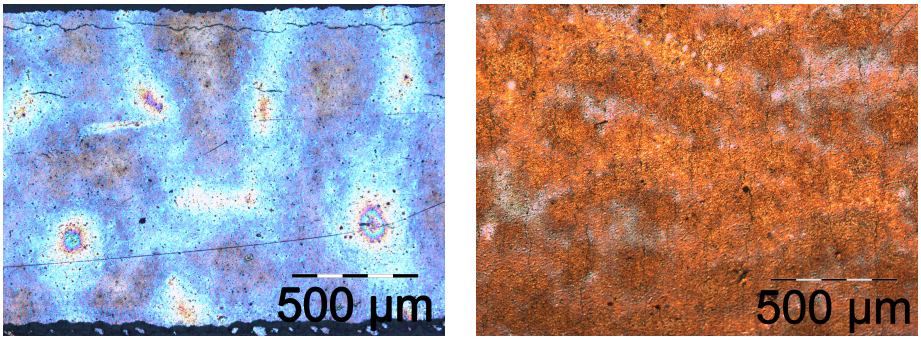

a b

Fig. 3. *Microscope images of printed traces on THERMLfilm substrate.*
a Aluminium trace
b Copper trace

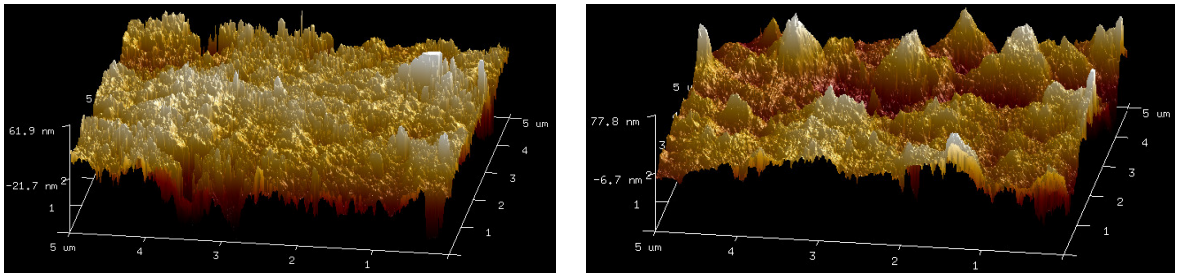

a b

Fig. 4. *AFM images showing the surface roughness of thermal-transfer printed traces on THERMLfilm.*
a Aluminium trace surface morphology
b Copper trace surface morphology

4. RFID tag design

Three different UHF RFID tag antenna designs were chosen to highlight the benefits and limitations of the printing techniques. As shown in Fig. 5, the antenna designs have different geometries featuring wide and narrow tracks that experience different conductor losses and are expected to have different read ranges. By using three different tags, we reduce the influence of any individual antenna design upon the results. In all cases, we used only a single printing pass.

NXP UCODE G2iL series RFID integrated circuits (IC) were attached to each of the fabricated antennas using conductive silver epoxy (Circuit Works CW2400) on the manufacturer-mounted

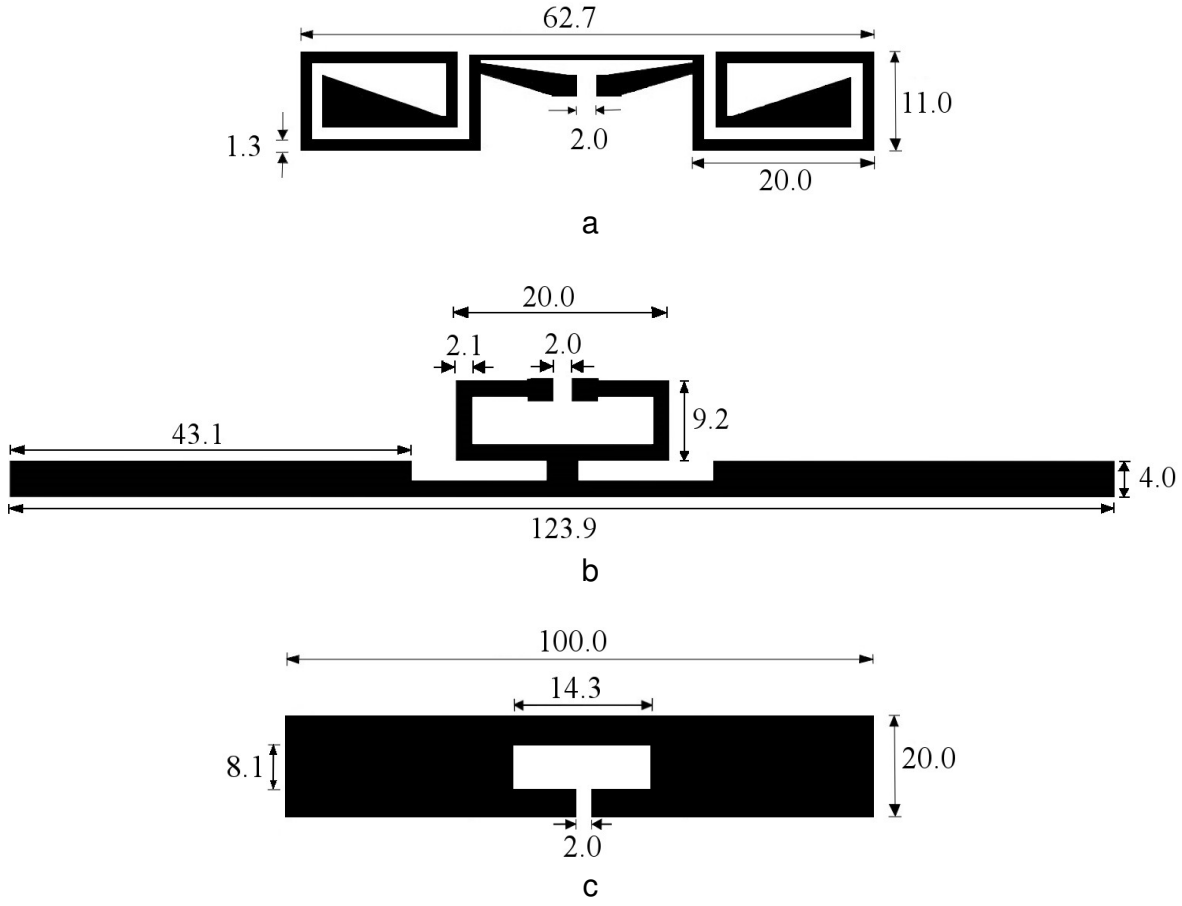

Fig. 5. *Schematics of the RFID tags. All dimensions in millimetres.*
a Tag design 1
b Tag design 2
c Tag design 3

fixture with two 3x3 mm^2 pads. After the attachment, the tags were placed in oven from 10 minutes at 70 °C to dry the silver epoxy. The read range of the tags was measured in a 120x80x80 cm Voyantic RFID measurement cabinet (Anechoic Chamber) using a Voyantic Tagformance RFID measurement unit. The equipment calculates the theoretical read range d from the backscattered signal from the tag assuming a reflection-less environment :

$$d = \frac{\lambda}{4\pi}\sqrt{\frac{EIRP}{P_{th}L_{iso}}}, \tag{1}$$

where λ is the wavelength of the transmitted signal to the tag, P_{th} is the measured threshold power

required to activate the tag, L_{iso} is the measured path loss, and $EIRP$ is the effective isotropically radiated power which is limited to 3.28 W according to the European regulations [25]. The RFID antenna reader has a linearly polarised patch antenna with 8 dB gain operating at 800-1000 MHz. The reader's output power ranges from 0 dBm to 27 dBm and the RF receiver has sensitivitiy of -75 dBm. The power was ramped up in 0.1 dBm steps until the tag is activated.

5. Simulation Results

The RFID antennas mentioned in the previous section were characterised using ANSYS high frequency structure simulator (HFSS) to estimate their read range. The material properties outlined in Table 3 were used to simulate the performance of each antenna design. THERMLfilm and Kapton films were modelled as 50 μm thick substrates with relative dielectric constants of 3.2 and 3.0 respectively. The conductive tracks of the antennas were modeled using the layered impedance boundary in HFSS. A lumped port with 50 Ω source impedance was used as excitation at antenna terminals. Read range of the tag was computed using the expression,

$$R_{range} = \left(\frac{\lambda}{4\pi}\right)\sqrt{\frac{\tau \cdot G_{Tg} \cdot EIRP}{P_{chip}}}, \tag{2}$$

where λ is the wavelength, τ is the power transmission coefficient, G_{Tg} is the gain of the tag, $EIRP$ is the equivalent isotropic radiated power and P_{chip} is the minimum power required to wake up the microchip. The power transmission coefficient depends on the antenna input impedance and the input impedance of the microchip as shown by the expression,

$$\tau = \frac{4R_A R_C}{(R_A + R_C)^2 + (X_A + X_C)^2}, \tag{3}$$

where $R_A + jX_A$ is the complex input impedance of the antenna and $R_C + jX_C$ is the complex input impedance of the chip. The equivalent circuit model of the NXP microchip developed in [27] was used to obtain the chip impedance across various frequencies.

The read range estimates computed using Equation (2) are plotted against frequency as shown in Fig. 6*a*, 6*b*, and 6*c* for tag design 1, design 2 and design 3 respectively. From the simulations, inkjet printed silver and thermal transfer printed aluminium on THERMLfilm substrate are expected to have very similar read range for all the tag designs. Inkjet printed silver on Kapton surface has the highest estimated read range, which is due to its higher thickness though its conductivity is lower. Thermal printed copper is expected to have a comparable albeit lower read range to inkjet printed silver on Kapton.

6. Measurement Results

The average theoretical read range of tag design one fabricated by the two printing methods is presented in Fig. 7. TTP copper antennas on THERMLfilm achieve a maximum read range of 6.6 m, while TTP aluminium antennas achieve 4.4 m read range. The difference of 2.2 m in the read range between the copper and aluminium TTP antennas is attributed to the higher conductivity of the copper traces and a thicker metalisation profile. These properties together with the narrow tracks of the antenna design results in significant conductor losses in the aluminium antennas and results in shorter average read range. The inkjet printed antennas on Kapton achieves a maximum read range of 5.9 m at 930 MHz. Inkjet printed antennas of THERMLfilm achieves a read range of 4.2 m, which is a 1.7 m less than the baseline performance. The difference is due to the suboptimal printing surface which results in thinner metalisation profile due to absorption of ink. The narrow metal tracks of the antenna design magnify the effects of the thin metalisation by increasing the ohmic losses, resulting in the significant reduction in reading range. The copper TTP antennas manages an improvement of 0.8 m in read range over the inkjet antenna on Kapton.

The average read ranges of antenna design two are shown in Fig. 8. The printed examples all achieve relatively similar read range, which we attribute to the thick lines of the design reducing the conductor losses and masking the difference in conductivity. Inkjet printed tags on THERML-film achieves 7.9 m read range which is 0.7 m less than the baseline due to the afore-mentioned suboptimal substrate properties. Aluminum TTP antennas on THERMLfilm achieve a read range of 7.7 m, which is similar to inkjet on THERMLfilm with a difference of 0.2 m. The copper TTP

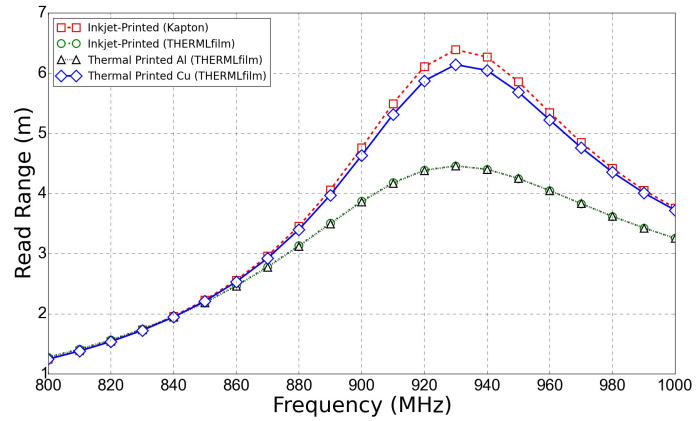

a

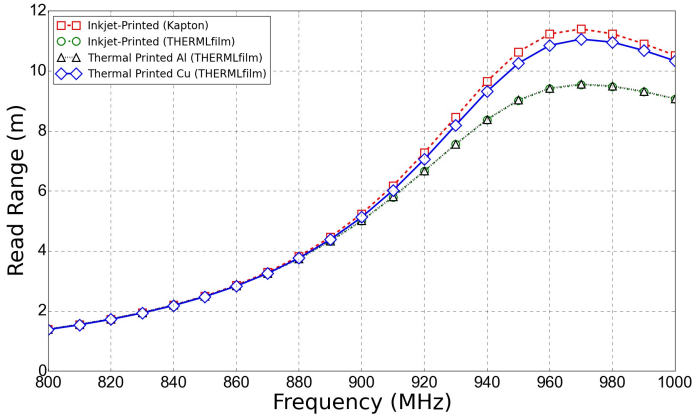

b

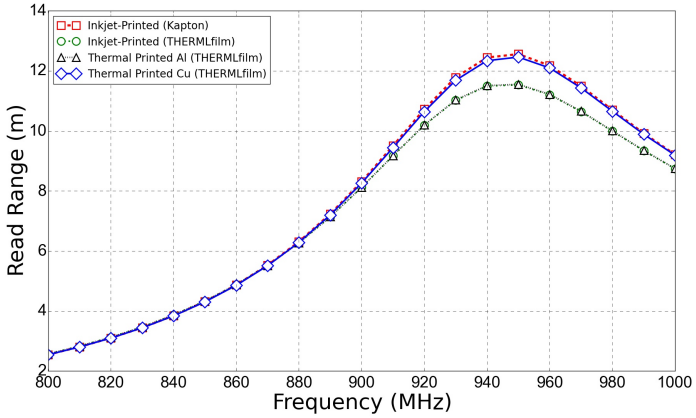

c

Fig. 6. *Simulated read ranges for antennas using material properties in Table 3*
a Tag design 1
b Tag design 2
c Tag design 3

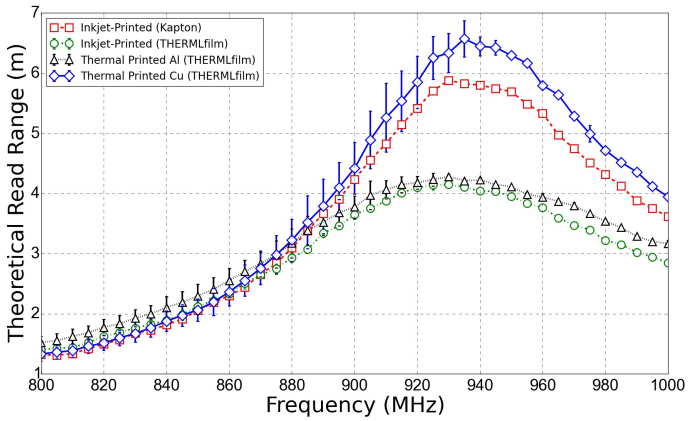

Fig. 7. *Measured theoretical reading range of tag design 1 fabricated by inkjet and thermal transfer printing methods*

antennas on THERMLfilm achieve peak read range of 9.0 m which is 0.4 m more than the inkjet printed antenna on Kapton. The inkjet on Kapton antennas achieve a maximum read range of 8.6 m at 960 MHz. The performance improvement of TTP copper over the baseline inkjet read range is due to the higher conductivity of the copper traces (see Table 3).

The average read range of tags of design three are shown in Fig. 9. There is more spread in the read range (2.3 m), similar to design one (1.2 m) due to the narrow and longer metal traces highlighting the effects of the conductor losses. Inkjet printed tags on THERMLfilm achieve a maximum read range of 9.2 m which is 1.6 m less than the baseline due to the suboptimal substrate. TTP aluminium antennas on THERMLfilm achieve a peak read range of 9.8 m, while the TTP copper antennas on THERMLfilm achieve a peak read range of 10.6 m. The inkjet tags on Kapton achieves a maximum read range equal to TTP copper tags on THERMLfilm of 10.6 m at 930 MHz.

A summary of the measured maximum read ranges is presented in Table 4. The achieved maximum theoretical read ranges by aluminium TTP antennas is equal to inkjet printing on THERMLfilm for the three designs in this study. The copper ribbon achieves better read range due a higher conductivity and a thicker metalisation compared to the aluminium ribbon leading to lower con-

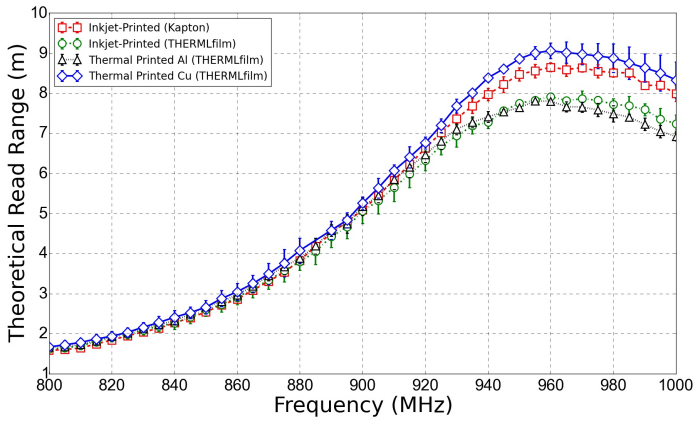

Fig. 8. *Measured theoretical reading range of tag design 2 fabricated by inkjet and thermal transfer printing methods*

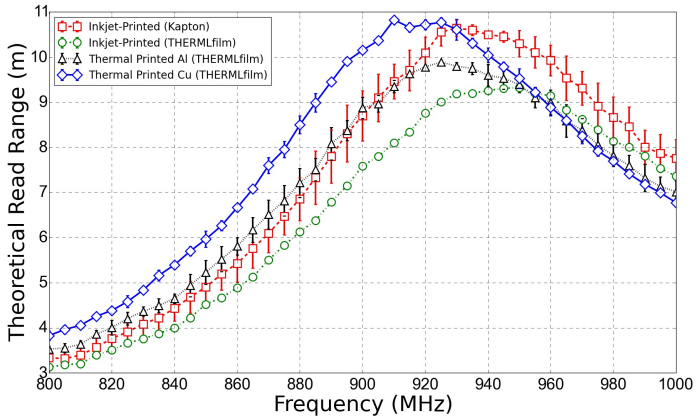

Fig. 9. *Measured theoretical reading range of tag design 3 fabricated by inkjet and thermal transfer printing methods*

ductor losses, which gives an overall performance similar to inkjet on Kapton. The simulation results suggest that inkjet printing on Kapton could be slightly better than thermal transfer printing with copper, but these simulations do not take into account all of the fabrication parameters due to modelling the metallised regions with idealised smooth surfaces and edges. In the measurements, where all practical effects are included in the results, the thermal transfer printed tags outperform the inkjet printed labels by between 15-60 % (1-10 %) compared to inkjet printing on THERMLfilm (Kapton).

Table 4 Measured Theoretical Read Range

Printing Method and substrate	Measured Theoretical Read range (m)		
	tag design 1 (940 MHz)	tag design 2 (960 MHz)	tag design 3 (920 MHz)
Thermal Transfer Printing (Al)			
THEMLfilm	4.4	7.7	9.8
Thermal Transfer Printing (Cu)			
THEMLfilm	6.6	9.0	10.6
Inkjet (Ag)			
THEMLfilm	4.2	7.9	9.2
Kapton	5.8	8.6	10.6

7. Conclusion

We fabricated UHF RFID tags and determined the maximum read range from measurements. By using different metal printing techniques, but keeping the tag antenna designs, electronic circuitry and substrate the same, we were able to separate out the influence of the printing method on the overall performance. We were primarily interested to see whether thermal transfer metal printing could produce acceptable performance, compared with inkjet printing. Our results indicate that thermal transfer printing using copper is able to equal or outperform inkjet printing with silver inks, regardless of whether the ink jet printing was conducted on the same substrate as the thermal printing, or on a substrate specially developed for inkjet printing. Our study used three different tag designs, representing antennas with a mix of thick and thin features, and more than one example was printed in most cases. Across the three designs, the thermal transfer printed labels outperform the inkjet printed labels by between 15-60 % (1-10 %) compared to inkjet printing on THERMLfilm (Kapton). Therefore our results justify further investigation of the use of thermal transfer printing in the production of UHF RFID tags in specific, and also indicate that it potentially has a role to play in printed electronics more generally. Thermal transfer printing is an attractive alternative to inkjet printing because it does not require sintering, thus eliminating an additional step from the tag fabrication process, saving time and money. There are opportunities for future work in the area of multiple-pass thermal transfer printing, establishing the fine resolution printing limits, and automating the assembly of printed structures that incorporate electronic elements, such

as switching elements that permit antenna reconfigurability [26].

Acknowledgment

The authors would like to thank Daniel Harrison from IIMAK for donation of both the aluminum and copper Metallograph^{TM} ribbons. This work was partly supported by European Commission from the Seventh Framework Programme through (FP7) AdvIOT (www.adviot.eu) and the Academy of Finland, Emil Aaltonen Foundation and TEKES.

8. References

[1] Tan, L. and Wang, N.: 'Future Internet: The Internet of Things', *Adv. Comp. Theory and Eng. (ICACTE), Aug. 2010 3rd Int. Conf.*, Chengdu, China, Aug. 2010, **5**, pp. 476-380.

[2] Harmon, R.R., Castro-Leon, E.G., Bhide, S.: 'Smart cities and the Internet of Things,' *Man. of Eng. and Tech. (PICMET)*, Portland, OR, USA, Aug 2015, pp. 485-494,

[3] Miorandi, D., Sicari, S.,De Pellegrini, F., Chlamtac, I.: 'Internet of things: Vision, applications and research challenges', *Ad Hoc Networks*, 2012, **10**,(7), pp. 1497-1516.

[4] Stankovic, J.A., 'Research Directions for the Internet of Things,' *Internet of Things Journal, IEEE* , 2014, **1**, (1), pp. 3-9,

[5] Gubbi, J., Buyya, R., Slaven Marusic, S., Marimuthu Palaniswami, M.: 'Internet of Things (IoT): A vision, architectural elements, and future directions', *Future Gen. Comp. Sys.*, 2013, **29**, (7), pp. 1645-1660,

[6] Wu, G., Talwar, S., Johnsson, K., Himayat, N., Johnson, K.D.: 'M2M: From mobile to embedded internet,' *Comm. Mag., IEEE* , 2011, **49**, (4), pp.36-43.

[7] Mantysalo, M., and Mansikkamaki, P.: 'An Inkjet-Deposited Antenna for 2.4GHz Applications', *AEU- Int Jrnl. of Elec. and Comms.*, 2009,**63**,(1), pp. 31-35.

[8] Batchelor, J.C., Parker, E.A., Miller, J.A., Sanchez-Romaguera, V., Yeates, S.G.: 'Inkjet printing of frequency selective surfaces,' *Electronics Letters*,2009, **45**, (1), pp. 7-8

[9] Redinger, D., Molesa, S., Shong Y., Farschi, R., and Vivek, S.: 'An ink-jet-deposited passive component process for RFID,' *Electron Dev., IEEE Trans.*, 2004 , **51**, (12), pp. 1978-1983.

[10] Kim, S., Cook, B., Taoran L., Cooper, J., Hoseon L., Lakafosis, V., Vyas, R., Moro, R., Bozzi, M., Georgiadis, A., Collado, A., Tentzeris, M.M.: 'Inkjet-printed antennas, sensors and circuits on paper substrate,' *Microwaves, Ant. & Pro., IET*, 2013 , **7**, (10), pp. 858-868.

[11] Virtanen, J., Virkki, J., Ukkonen, L., Sydänheimo, L.: 'Inkjet-Printed UHF RFID Tags on Renewable Materials,'*Adv. Internet of Things*, 2012, **2** (4), pp. 79-85.

[12] Zhou, J., Ge T., Ng, E., Chang, J.S.: 'Fully Additive Low-Cost Printed Electronics With Very Low Process Variations,' *Electron Devices, IEEE Trans.*, 2016, **63**, (2), pp. 793-799.

[13] Merilampi, S., Björninen, T., Ukkonen, L., Ruuskanen, P., Sydänheimo, L.,:'Embedded wireless strain sensors based on printed RFID tag', *Sensor Review*, 2011, **31**,(1) , pp. 32-40.

[14] Kgwadi, M., Vourch, C.J., Harrison, D.J., Drysdale, T.D.: 'On-demand printing of antennas for TV white-space communications,' *Ant. and Prop. Conf. (LAPC)*, Loughborough, UK., Nov. 2014, pp. 553-556.

[15] Whyte, G., Harrison, D., Cumming, D., and Drysdale, T.: 'Direct Printing of Flexible Metallic Millimetre-wave Frequency Selective Surfaces', *Anten. and Prop. Soc. Int. Symp. (APSURSI)*, Toronto, ON, Canada, July 2010, pp. 1-4.

[16] Arora, N. D. :'Modeling and characterization of copper interconnects for SoC design,' *Sim. of Semiconductor Processes and Devs., SISPAD 2003. Intl. Conf.*, Boston, MA, USA, 2003, pp. 1-6.

[17] Merilampi, S. L., Björninen, T., Ukkonen, L., Ruuskanen, P., and Sydänheimo, L.:'Characterization of UHF RFID tags fabricated directly on convex surfaces by pad printing' , *Int. Jrnl. of Adv. Manuf Technol*, 2011, **53**(5), pp. 557-591.

[18] Hicks, W. T., Allington, T. R., and Johnson,V.: 'Membrane Touch switches: Thick-Film Materials Systems and Processing Options,' *IEEE Trans. on Components, Hyb., and Manuf. Tech.*,1980, **3**,(4), pp. 518-524,

[19] Salmeron, J.F., Molina-Lopez, F., Briand, D., Ruan, J.J., Rivandeneyra, A., Carvajal, M.A., Capitan-Vallvey, L.F., Derooij, N.F., and Palma, A.J.:'Properties and Printability of Inkjet and Screen-Printed Silver Patterns for RFID Antennas' , *Jrnl. of Elect. Materials*, 2013, **43**(2), pp. 604-617 .

[20] 'Product Construction Sheet', http://www.uce-druckservice.de/downloads/flexcon/select/THERMLfilm%20Select%2021944E.pdf, accessed 20 January 2016

[21] Virkki, J., Virtanen, J., Sydänheimo, L., Ukkonen, L., Tentzeris, M.: 'Embedding inkjet-printed antennas into plywood structures for identification and sensing,' *RFID-Tech. and App. (RFID-TA)IEEE Intl. Conf.* , Nice, France, Nov. 2012, pp. 34-39.

[22] 'Nano Paste Series', https://www.harima.co.jp/en/products/electronics/pdf/brochure16e_23.pdf, accessed 20 January 2016

[23] Ren, Y., Virkki, J., Sydänheimo, L., Ukkonen, L., 'Optimisation of manufacturing parameters for inkjet-printed and photonically sintered metallic nanoparticle UHF RFID tags,' *Elec. Let.*, 2014, **50**, (21), pp. 1504-1505.

[24] Timoshevskii, V., Ke, Y., Guo, H., Gall, D.:'The influence of surface roughness on electrical conductance of thin Cu films: An ab initio study' , *Jrnl. of Applied Phys.*, 2008 **103**.

[25] 'ETSI TR 101 445 v1.1.1 (2002-04)' http://www.etsi.org/deliver/etsi_tr/101400_101499/101445/01.01.01_60/tr_101445v010101p.pdf, accessed 14 February 2016.

[26] Kgwadi, M., Drysdale, T. D.: 'Diode-switched thermal-transfer printed antenna on flexible substrate', *IET Electronics Letters*, 2016, **54**, (4), pp. 258-260.

[27] Björninen, T., Syndänheimo, L., Ukkonen, L.: 'Development and validation of an equivalent circuit model for UHF RFID IC based on wireless tag measurements', *Digest of AMTA Symp.*, Bellevue, WA, USA, Oct. 2012, pp 480-485.